

The Effect of Instrument Polarization Sensitivity on Sea Surface Remote Sensing with Infrared Spectroradiometers

JOSEPH A. SHAW

Department of Electrical and Computer Engineering, Montana State University, Bozeman, Montana

(Manuscript received 30 August 2000, in final form 12 October 2001)

ABSTRACT

The sensitivity of Fourier transform infrared spectroradiometers to the polarization state of incident radiance can become significant in radiometric measurements of a partially polarized source such as the sea surface. At off-nadir incidence angles and wavenumbers below about 2750 cm^{-1} (wavelengths longer than $3.6 \mu\text{m}$), radiance from the sea surface is partially vertically polarized, because the vertically polarized sea surface emission exceeds the horizontally polarized background reflection. At larger wavenumbers (wavelengths shorter than $3.6 \mu\text{m}$), reflected skylight becomes more significant, and the total radiance at off-nadir angles can become horizontally polarized. This paper shows how the inherent polarization sensitivity ($\sim 5\%$) of a typical Fourier transform infrared instrument leads to radiometric errors that are small ($\sim 0.1 \text{ K}$) but significant for radiometrically demanding sea surface remote sensing applications at large incidence angles. For incidence angles below approximately 45° , the polarization-induced error for longwave infrared measurements typically is less than approximately 0.05 K and therefore often can be neglected in sea surface radiometry. However, in polarimetric measurements used, for example, to increase contrast between man-made objects and the background, the instrument polarization sensitivity must be considered always.

1. Introduction

Infrared radiance from the sea surface can be significantly polarized when measured at large incidence angles (Shaw 1999). Because incidence angles of 50° or more are common for ship-mounted radiometers (Minnett et al. 2001; Donlon et al. 1998; Wu and Smith 1997; Suarez et al. 1997; Smith et al. 1996; Schluessel et al. 1990), the polarization sensitivity of these radiometers becomes important. In some cases, radiometers with a vertical polarizer have been pointed at the Brewster angle to eliminate the reflected atmospheric radiance from the measurement (e.g., Suarez et al. 1997), although consistently accurate results are not practical with this approach because of the difficulty in keeping the radiometer pointed at the Brewster angle throughout the instrument's optical bandwidth on a moving ship with a rough sea. The majority of the time, however, polarizers are not used, and the radiometer is assumed to have no polarization sensitivity. Nevertheless, this is not always true, especially for instruments that use gratings, beam splitters, or other components whose optical properties vary with the polarization state of incident radiance.

In some cases, of primarily military interest, the infrared radiance is measured or calculated polarimetrically to increase contrast between man-made objects and the background (Egan 2000; Fetrow et al. 2000; Howe et al. 2000; Zeisse et al. 1999; Cooper et al. 1996). These measurements rely on a difference in polarization state between the target and the background, or quite often even assume that the background is unpolarized. In such cases where polarization is being measured directly, the instrument polarization sensitivity always must be considered carefully.

Fourier transform infrared (FTIR) spectroradiometers are being used increasingly often in the environmental and military remote sensing communities for measuring infrared spectral radiance and spectral polarization (Minnett et al. 2001; Fetrow et al. 2000; Shaw 2001; Shaw et al. 1999; Wu and Smith 1997; Smith et al. 1996). FTIR instruments use beam splitters and mirrors that usually favor one polarization state over another, creating an instrument polarization sensitivity that can cause errors in radiometric measurements of partially polarized radiance when the instrument is calibrated with unpolarized sources. The potential for polarization errors contributing significantly to the error budget of modern infrared satellite sensors also has been recognized, particularly because of polarization-dependent scan mirrors and gratings (Pagano et al. 2000; Gigioli and Pagano 1999; Knight et al. 1999). This issue is complicated by the variability of the scene polarization

Corresponding author address: Dr. Joseph A. Shaw, Electrical and Computer Engineering Dept., Montana State University, 610 Cobleigh Hall, Bozeman, MT 59717-3780.
E-mail: jshaw@ece.montana.edu

with the radiometer's incidence angle, water surface roughness, atmospheric conditions, and so forth. Therefore, because the state of polarization is not always simple to predict, its impact on the error budget for radiometric measurements should not be neglected without careful consideration.

2. Infrared sea surface polarization

Infrared sea surface radiance is predominantly vertically polarized at wavenumbers below about 2750 cm^{-1} (wavelengths longer than $3.6 \mu\text{m}$) and horizontally polarized at higher wavenumbers (shorter wavelengths) (Shaw 1999). To see why this is so, consider the radiance measured by an ocean-viewing radiometer as the sum of surface emission, reflected background radiance, and atmospheric path radiance:

$$L(\bar{\nu}, \theta) = \tau_a(\epsilon L_w + RL_{bg}) + L_a, \quad (1)$$

where $L(\lambda, \theta)$ is the spectral radiance measured at wavenumber $\bar{\nu}$ and angle θ , ϵ is the sea surface emissivity, L_w is the blackbody radiance at the water surface temperature, R is the water surface reflectivity, L_{bg} is the background atmospheric radiance (including direct or scattered radiance from the sun, clouds, atmospheric thermal emission, and so on), L_a is the radiance emitted by the atmospheric path between the radiometer and the water surface, and τ_a is the atmospheric transmittance for the path between the radiometer and water surface. Each component of Eq. (1) depends on wavenumber $\bar{\nu}$ and incidence angle θ (with respect to the water surface normal), while only the atmospheric-path emission and transmittance terms usually do not depend on polarization at thermal infrared wavenumbers. The key to understanding the polarization state of sea surface radiance is to recognize that the surface emissivity ϵ in Eq. (1) is equal to one minus the reflectivity (true for any medium with zero net transmittance), which causes the surface-emission and background-reflection terms to be complementary in magnitude and polarization orientation.

The complementary relationship between emissivity and reflectivity has a large influence on the state of polarization in infrared ocean measurements. Whereas the reflected radiance tends to be horizontally polarized, the emitted surface radiance is vertically polarized. A simple conceptual picture to consider is the emission polarization arising from refraction of initially unpolarized thermal radiance as it is transmitted through the water-air interface at an oblique incidence angle (Millikan 1895; Sandus 1965). Therefore, emission polarization is proportional to the Fresnel transmissivity of the water-air interface, which favors vertical polarization at oblique angles, while reflection polarization is proportional to the Fresnel reflectivity, which favors horizontal polarization.

The net polarization state of an ocean scene depends primarily on the radiometric contrast between the or-

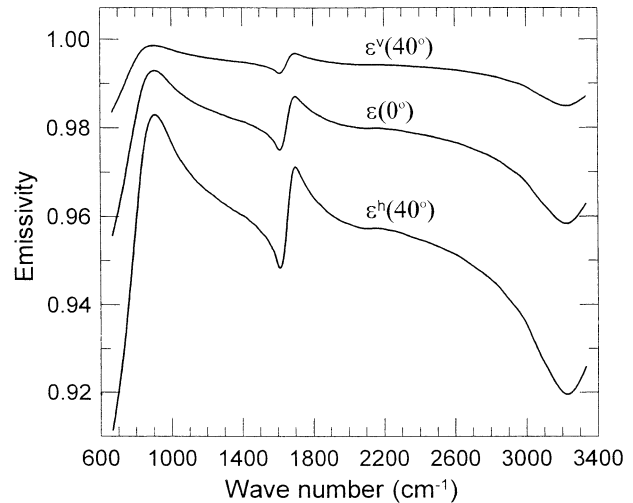


FIG. 1. Infrared spectral emissivity of water for incidence angles of 0° (normal) and 40° . As the incidence angle increases, the emissivity polarization components diverge, with the horizontally polarized component below the normal-incidence value and the vertically polarized component above. Beyond the Brewster angle, both components decrease.

thogonally polarized water-emission and background-reflection terms. For a horizontally oriented sea surface, the degree of linear polarization can be written as

$$dp = \frac{L^h - L^v}{L^h + L^v}, \quad (2)$$

where L^h is the horizontally polarized radiance and L^v is the vertically polarized radiance. The degree of polarization has a magnitude between 0 and 1, indicating totally unpolarized and polarized light, respectively, with a sign that is positive for horizontal and negative for vertical polarization.

The degree of linear polarization in sea surface radiance increases with incidence angle as the polarization components of emissivity diverge, as shown in Fig. 1. However, the overall decreasing magnitude of the emissivity at larger incidence angles means that the reflectivity increases. Consequently, near 80° the degree of polarization curve usually reverses and becomes rapidly smaller, as shown in Fig. 2, for a longwave (1100 cm^{-1}) and shortwave channel (3270 cm^{-1}).

Figure 3 shows the degree of polarization calculated as a function of wavenumber from the formulation of Eqs. (1) and (2) with a clear 1976 U.S. Standard Atmosphere model and a smooth sea surface viewed at 75° incidence angle (relative to the surface normal) from a 10-m height (Shaw 1999). Relative to this spectrum, the degree of polarization is reduced by approximately half at 60° and by approximately one-fourth at 45° . Figures 2 and 3 both demonstrate that sea surface polarization is often positive for wavenumbers above about 2760 cm^{-1} and usually negative below 2760 cm^{-1} . At low wavenumbers, the sea surface typically exhibits net negative polarization because the surface emission dom-

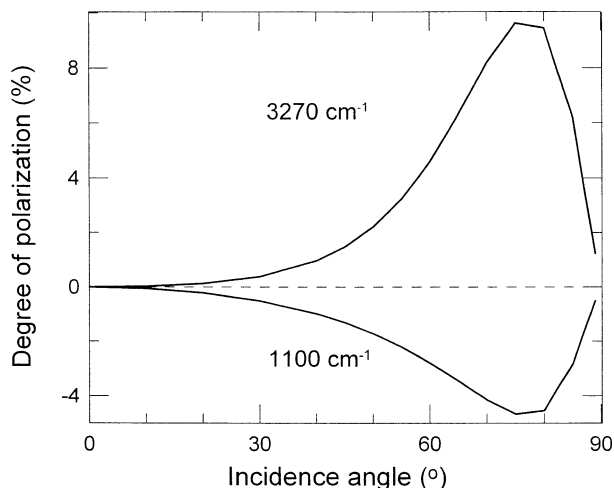


FIG. 2. Degree of polarization (%) vs incidence angle for sea surface radiance viewed from 10-m height under a 1976 U.S. Standard Atmosphere for wavenumbers of 1100 and 3270 cm^{-1} . These curves show typical positive polarization for large wavenumbers and negative polarization for small wavenumbers.

inates the background reflection. Conversely, at larger wavenumbers the amount of scattered sunlight during the day is strong enough to increase the reflected-background atmosphere component sufficiently that it dominates the water-emitted radiance, resulting in a net positive (horizontal) polarization state. This kind of polarization signature has been measured (Cooper et al. 1996), but the exact amount of positive polarization in the shortwave infrared spectral region depends strongly on atmospheric particulate scattering (Shaw 1999).

The polarization spectrum in Fig. 3 includes the two primary atmospheric window regions of approximately 700–1300 cm^{-1} and 2000–3300 cm^{-1} , where the atmosphere is relatively transparent. The emission polarization for water is strongest within these two window regions, but between them low atmospheric transmittance leads to weak polarization, because the sea surface emission term is reduced by the intervening atmosphere. Similarly, the entire spectrum shows atmospheric emission and absorption features, resulting from a combination of absorption of the surface-emitted radiance in the intervening atmosphere and reflection of atmospheric emission from the sea surface.

The degree of polarization increases with radiometric contrast between the sea surface and the reflected background (absorption by the intervening atmosphere is also significant, especially for long viewing paths). Thus, the sea surface viewed under a radiometrically bright cloud, or through a humid atmosphere, exhibits less polarization than the same surface viewed under a clear, dry atmosphere. Wind-induced surface roughness tends to slightly decrease the polarization at incidence angles below about 70° and increase it at larger angles. Sun and moon glints add positive (horizontal) polarization, with even tiny amounts (~1%) of sun glint in

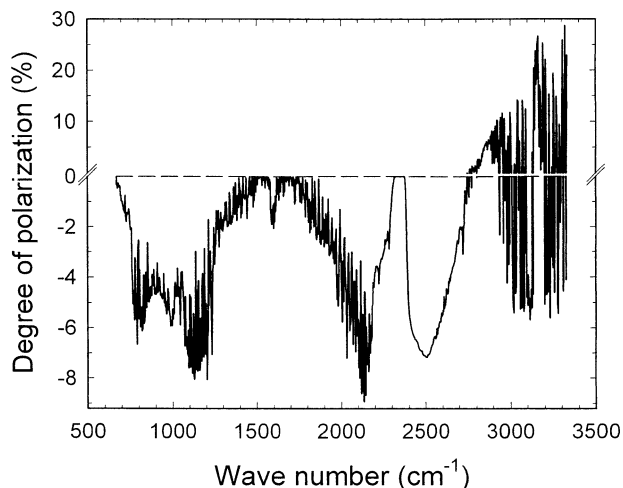


FIG. 3. Spectral degree of polarization (%) for a smooth sea surface viewed under the same environmental conditions as Fig. 2 and an incidence angle of 75°. Note the scale break on the vertical axis.

the beam capable of reversing the sign of the polarization signature from negative to positive throughout the spectrum. The dependence of sea surface polarization on these and other conditions as a function of wavelength has been described with more detail in Shaw (1999).

3. FTIR spectroradiometer polarization sensitivity

The polarization sensitivity of a popular FTIR spectroradiometer (Bomem MR100) was determined by measuring radiance spectra of an unpolarized blackbody source through a wire-grid polarizer. This same kind of FTIR instrument is often used for measuring atmospheric and oceanic emission (Minnett et al. 2001; Shaw et al. 1999; Wu and Smith 1997; Smith et al. 1996), and its potential for polarization sensitivity is not fundamentally different from that of FTIR instruments made by other manufacturers. The polarization response of this particular instrument was found to be approximately -5% throughout the spectral region of 700–1400 cm^{-1} , where local atmospheric fluctuations cause minimal interference (the minus sign indicates that the instrument response is higher for vertical polarization).

These measurements used three separate blackbody sources: a test target at 310 K, and radiometric calibration sources at 290 and 330 K. All three sources have honeycomb surfaces, with thermoelectric temperature control to ± 0.1 K, and emissivity specified at 0.996 or greater. These same sources are used in field measurements of atmospheric emission that require strict radiometric accuracy. Atmospheric emission data from this same FTIR instrument with the same calibration sources, usually with 20–30 averaged scans at each target (cold blackbody, warm blackbody, and sky) with 1 cm^{-1} spectral resolution, have been shown to repeatedly have an uncertainty that is less than 1% of ambient blackbody

radiance (Shaw et al. 1999). These calibration sources have been used for a variety of infrared polarization experiments also, with consistent evidence of having no measurable polarization.

Although field measurements usually use a beam-steering mirror at the front of the FTIR, the polarization measurements described here were made without this mirror by positioning each blackbody target sequentially in front of the FTIR aperture. Keep in mind that a beam-steering mirror oriented at 45° to direct sea surface emission into a horizontal instrument will increase the instrument sensitivity to vertical polarization by approximately 0.5%–1.5%, which needs to be considered in interpreting the results shown in this paper for no beam-steering mirror. The ZnSe window that normally covers the FTIR aperture was replaced by a wire-grid polarizer with a ZnSe substrate. Experiments using a variety of acquisition times and spectral resolutions led to the choice of 10 scans per target with 16 cm^{-1} spectral resolution. This choice is a good compromise between averaging longer to obtain high signal-to-noise ratio and maintaining short measurement times to avoid drift in the instrument or the atmosphere. The spectral resolution choice was governed by a similar compromise, but between using fine resolution to look for meaningful spectral structure in the polarization response and using coarse resolution to obtain shorter measurement times (it turns out the FTIR polarization response has no obvious sharp spectral features). An added advantage of lower spectral resolution is that noisy fluctuations caused by highly absorbing atmospheric absorption lines are less apparent in the measurements.

Measuring the instrument's polarization sensitivity was done in two steps: 1) a long sequence of measurements at 15° increments of polarizer angle to establish the plane of preferred polarization, and 2) a faster sequence of measurements at the polarizer angles corresponding to maximum and minimum instrument response to measure the actual instrument polarization sensitivity function. The first sequence was performed by obtaining spectra at 15° increments of the polarizer angle from 0° to 360° for all three blackbody targets (at 290, 310, and 330 K). The total elapsed time for this sequence of measurements at all polarizer angles was approximately 55 min, quite a bit longer than our typical 15–20-min period between calibrations for atmospheric measurements, but still short enough to expect reasonably stable operation of the FTIR instrument inside a temperature-controlled laboratory. The second sequence at the maximum- and minimum-response angles required less than 10 min for completion each time it was repeated. The spectra of the 310-K source were calibrated with the 290- and 330-K blackbody spectra, using the 2-point complex calibration algorithm described by Revercomb et al. (1988). Using calibration measurements at each polarizer setting would remove the instrument polarization response; therefore, to provide a common reference for determining the polarization sen-

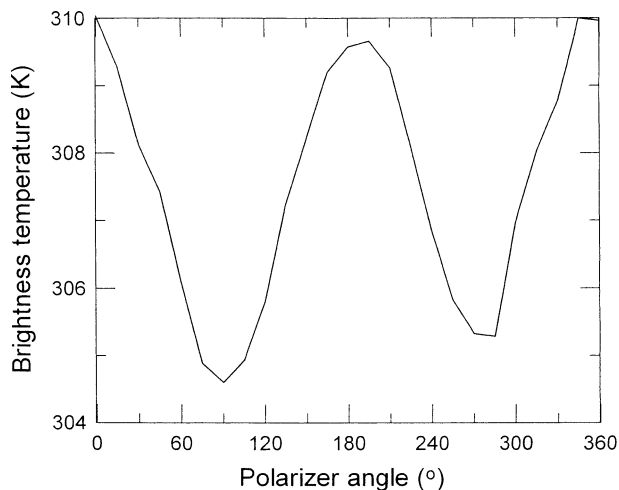


FIG. 4. Brightness temperature (K) response of the FTIR spectroradiometer as a function of polarizer angle for radiance from a 310-K blackbody calibration source. Measurements in 15° increments of polarizer angle were calibrated with reference spectra at a polarizer angle of 0° (a horizontal wire grid, which passes vertical polarization).

sitivity, spectra obtained with the polarizer at all angles were calibrated with the vertically polarized blackbody spectra (polarizer angle = 0°).

The FTIR polarization response is shown in Fig. 4 as a function of polarizer angle, for brightness temperature at 1050 cm^{-1} (0° corresponds to a horizontal wire grid, which passes vertical polarization). The signal maxima at 0° and 180° and minima at 90° and 270° indicate an instrument response that is strongest for vertical polarization and weakest for horizontal polarization. The correspondence of these maxima and minima to the instrument vertical and horizontal axes suggests that this sensitivity arises primarily at the beam splitter in the interferometer. This graph also displays a second-harmonic cosinusoidal variation, which suggests some misalignment of the polarizer with respect to the instrument's optical axis. The polarization response is similar throughout the spectral band of $700\text{--}1400\text{ cm}^{-1}$, with an average sensitivity of approximately $-5\% \pm 1\%$ [calculated as 100% times the degree of polarization given by Eq. (2) for radiance]. At higher and lower wavenumbers, atmospheric fluctuations made reliable measurements impractical.

Figure 5 shows brightness temperature difference spectra of the 310-K blackbody source viewed through the polarizer at different pairs of angular settings (from the long sequence described previously). Each curve is the difference between the spectrum with the polarizer oriented at 0° to pass vertical polarization and a spectrum with the polarizer at 45° , 90° , 180° , or 360° . This measurement sequence took long enough that changes occurred in the local air and in the instrument, resulting in some signal variations that are not related to polarization. The spectra are strongly affected by carbon dioxide absorption and emission at the low wavenumber

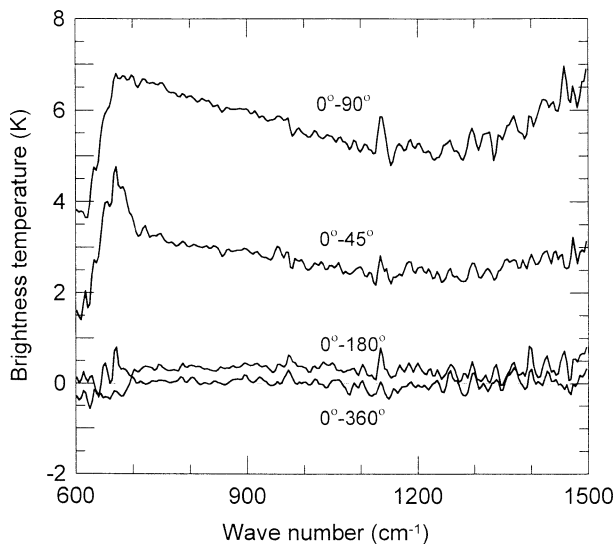


FIG. 5. Brightness temperature (K) vs wavenumber difference between spectra measured with the polarizer at 0° and spectra with the polarizer at the noted angle (45° , 90° , 180° , or 360°). The larger fluctuations at the low- and high-wavenumber ends of the spectra are caused by air temperature and humidity variations.

end ($\sim 600\text{--}700\text{ cm}^{-1}$), and by water vapor at the high wavenumber end ($\geq 1300\text{ cm}^{-1}$). However, the $0^\circ\text{--}360^\circ$ difference spectrum in Fig. 5 (which ideally would be zero) shows that, even with the long measurement time period, the rms difference is about 0.1 K throughout the window region of the spectrum ($\sim 700\text{--}1300\text{ cm}^{-1}$), and 2 or 3 times higher in more opaque bands near the ends of the spectrum shown. Also, the previously mentioned polarizer misalignment is the likely cause of the offset in the $0^\circ\text{--}180^\circ$ difference spectrum. The large mean differences between these curves (all more than an order of magnitude larger than the uncertainties) clearly illustrate the polarization sensitivity of the FTIR instrument, which reaches its maximum for the $0^\circ\text{--}90^\circ$ difference.

4. Effect of polarization sensitivity on sea surface radiometry

The impact of partially polarized radiance on radiometric measurements depends primarily on how the polarization alters the overall radiance and how the radiometer response varies with polarization. In fact, this relatively small instrument polarization sensitivity coupled with a similarly small amount of sea surface polarization does not present as big a problem in an application such as sea surface temperature (SST) radiometry as it does in a surveillance application where the polarization signature of a target is being measured (e.g., Egan 2000; Fetrow et al. 2000; Howe et al. 2000; Zeisse et al. 1999; Cooper et al. 1996). For these direct polarimetry problems, ignoring the instrument polarization sensitivity would result in an error that easily

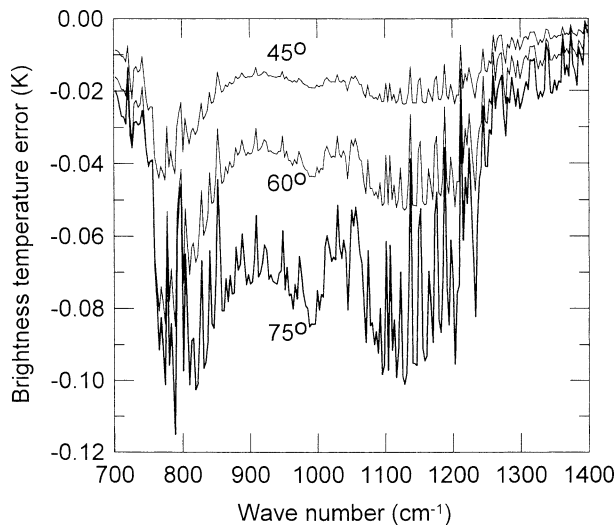


FIG. 6. Brightness temperature error (K) vs wavenumber that results from neglecting a -5% instrument polarization sensitivity in a sea surface measurement at 45° , 60° , and 75° incidence angle (with the same environmental conditions as Figs. 2 and 3). The error is calculated as an ideal measurement minus a measurement with the polarization-sensitive instrument.

could be as large as the measured polarization value. In nonpolarimetric sea surface measurements the effect is more subtle, but still can be important for high-accuracy radiometry at large angles of incidence.

Figure 6 shows the calculated brightness temperature error that results from neglecting the -5% instrument polarization sensitivity when a 295-K sea surface is viewed from a 10-m height through a 1976 U.S. Standard Atmosphere at viewing angles of 45° , 60° , and 75° . Specifically, the curves in this figure show the difference for a measurement using an ideal instrument minus a measurement with the -5% polarization sensitivity. This figure covers only the spectral range over which the FTIR polarization response was measured with minimal atmospheric fluctuations, as described in the previous section. In Fig. 7, the calculation for 75° is extended over the full thermal infrared spectral range of $667\text{--}3300\text{ cm}^{-1}$ ($3\text{--}15\text{-}\mu\text{m}$ wavelength) with a constant -5% polarization sensitivity. The vertical polarization sensitivity creates a larger apparent radiance in the spectral regions where the sea surface radiance is partially vertically polarized and a smaller apparent radiance for wavenumbers where the surface radiance is horizontally polarized. Thus, the differences are predominantly negative for small wavenumbers and positive for large wavenumbers.

The largest errors occur on the edges of the window regions of the spectrum (near 800, 1100–1200, 3100–3200, and 3300–3400 cm^{-1}). In fact, these spectral bands have the highest polarimetric errors for the same reasons that they are often used for remote sensing: they offer a combination of high surface emission and reasonably low atmospheric attenuation. At this large in-

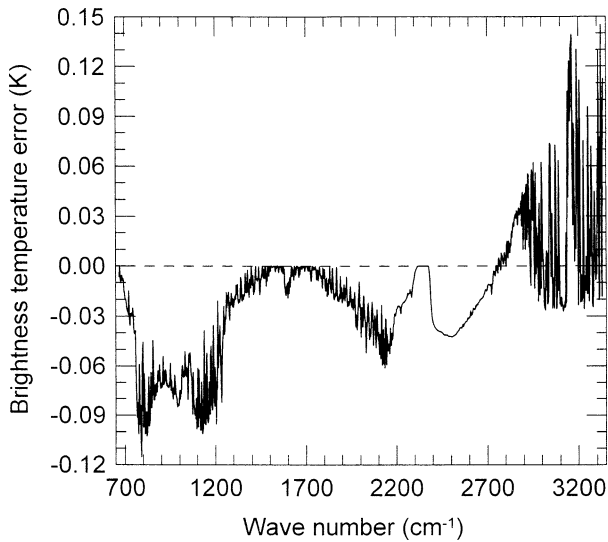


FIG. 7. Calculated brightness temperature (K) (radiometric) error vs wavenumber at 75°, as in Fig. 6 but over a larger spectral range.

incidence angle of 75°, the error with a -5% instrument polarization sensitivity exceeds 0.1 K near 800 and 1100 cm^{-1} , both spectral regions commonly used in remote sensing applications.

Figure 7 represents the incidence angle with approximately maximum polarization and, therefore, maximum polarization error. The variation of the radiometric error with incidence angle is indicated in Fig. 8, which plots the polarization-induced error in sea surface brightness temperature as a function of incidence angle at 789, 834, 900, 2700, and 2900 cm^{-1} . These spectral wavenumbers include the largest error from Fig. 6 (789 cm^{-1}) and four other wavenumbers that are included in common satellite sea surface temperature bands. The error at the largest wavenumbers reverses sign at angles greater than about 60°, beyond which the reflected atmospheric radiance dominates the direct surface emission. In the quest for increasingly high radiometric accuracy, the errors shown here for large incidence angles are significant. In fact, the errors are a significant fraction of (or even larger than, in some cases) the maximum total uncertainty of 0.1 K required for most modern sea surface radiometric measurements. Therefore, sea surface measurements with this kind of instrument at large incidence angles must consider the effect of polarization. Conversely, the errors for angles less than about 45° are mostly negligible. However, even if they are ignored, their magnitude should be considered in the overall error budget.

Validation of satellite SST measurements is one of the applications where this kind of polarization error can arise. Spectral channels used for satellite SST include approximately 800–870 and 890–980 cm^{-1} for the Geostationary Operational Environmental Satellite (GOES); 815–850, 887–928, 2451–2488, 2507–2545, and 2604–2732 cm^{-1} for the moderate-resolution im-

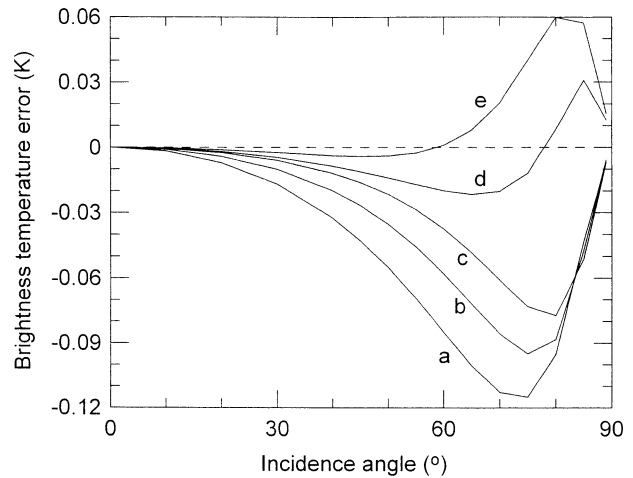


FIG. 8. Variation of the brightness temperature error (K) with incidence angle at (a) 789, (b) 834, (c) 900, (d) 2700, and (e) 2900 cm^{-1} . These frequencies represent (a) the maximum error and [(b)–(e)] the error at four typical SST bands for an instrument polarization sensitivity of -5% .

aging spectroradiometer (MODIS); and near 2700, 1231, and 900 cm^{-1} for the atmospheric infrared sounder (AIRS). Most of these spectral bands have polarization-induced errors of approximately 0.5–0.8 K in the 75° view of Fig. 7 but much smaller errors (≤ 0.3 K) below 50° (see Fig. 8).

The calculations shown previously all assume a 1976 *U.S. Standard Atmosphere* (Anderson et al. 1986), which has a water vapor mixing ratio of 7.75×10^3 ppmv (parts per million by volume) at the surface, decreasing with height. Atmospheric water vapor and clouds are the primary variable that can change the maximum degree of polarization in infrared sea surface radiance. For example, the more humid Tropical Atmosphere model (2.59×10^4 ppmv water vapor at the surface) leads to a polarization spectrum that has a similar shape to Fig. 3, but with a maximum amount of longwave polarization that is typically less than -3% (Shaw 1999). However, the polarization is higher in situations with less water vapor than the 1976 *U.S. Standard Atmosphere*. Examples of where this might happen include high-latitude oceans and continental lakes (in semiarid regions of the American West, for example, wintertime water vapor mixing ratios at the surface are commonly near 1×10^3 ppmv).

Sun glints (specular solar reflections) can lead to large polarization-induced radiometric errors. Figure 9 shows the error calculated at 60° incidence for an instrument with -5% polarization sensitivity viewing water with 1% of the field of view containing sun glints. The first obvious feature of this error spectrum is its positive sign, resulting from the dominant horizontal polarization created by the large reflected radiance. The next obvious feature is the large magnitude of the error, which results directly from the large magnitude of reflected radiance that exists with even a very small fraction of sun glint

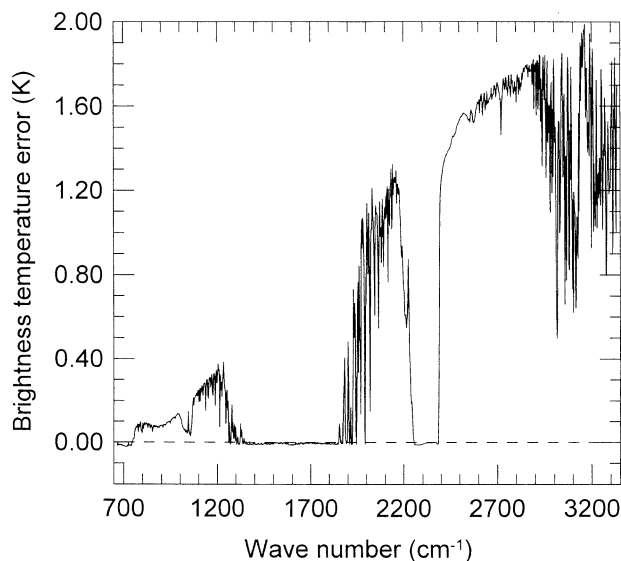


FIG. 9. Brightness temperature error (K) vs wavenumber spectrum for the conditions of Fig. 6 but at a 60° incidence angle, with sun glints occupying 1% of the sensor field of view.

in the radiometer beam (Shaw 1999). Other nonpolarimetric radiometric errors make SST measurements undesirable in the vicinity of sun glints, but some surveillance problems focus specifically on the high-clutter region near the solar specular angle (e.g., Egan 2000; Zeisse et al. 1999; Cooper et al. 1996). Moon glints are significantly weaker, but a similar effect can occur with 30% or more fractional coverage.

Also of practical value is the question of how high the instrument polarization sensitivity has to be to produce serious radiometric errors at modest incidence angles. Figure 10 shows the radiometric error calculated for a sensor with 20% polarization sensitivity, looking at 45° from a 10-m height through a 1976 *U.S. Standard Atmosphere*. Neglecting this large instrument polarization response results in longwave errors of the order 0.1 K even at this modest incidence angle. For a 75° angle the error increases to about 0.5–0.7 K in the longwave infrared region (~ 600 – 1500 cm^{-1}) and ± 0.3 K in the shortwave (~ 2400 – 3400 cm^{-1}) infrared spectral region. Such a large polarization sensitivity does, in fact, exist in the infrared channels of the AIRS grating spectroradiometer (Pagano et al. 2000; Gigioli and Pagano 1999).

The previous discussion shows that, for the particular FTIR instrument used here, accounting for the instrument polarization sensitivity is only necessary for measurements of water radiance at incidence angles above about 50° when the background sky is reasonably dry and clear, or whenever direct polarimetric measurements are desired. In many cases, with smaller angles or less radiometric contrast between the water and background, this relatively modest instrument polarization sensitivity can be neglected. Keep in mind, however, that a beam-

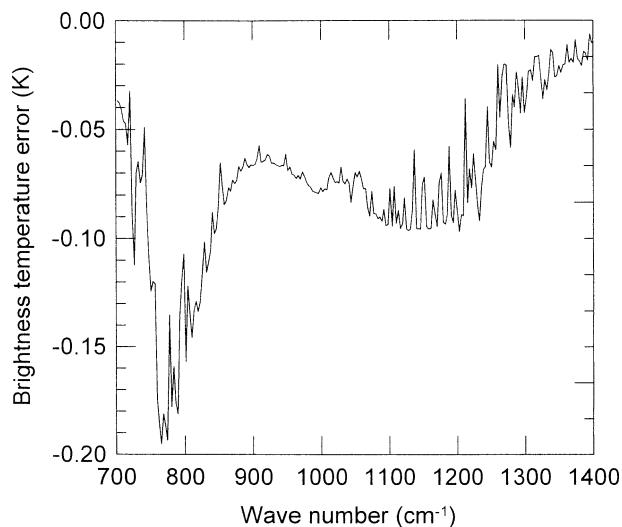


FIG. 10. Brightness temperature error (K) vs wavenumber spectrum for an instrument with 20% polarization sensitivity, viewing water at a 45° incidence angle.

steering mirror will increase the instrument polarization sensitivity beyond what has been shown here, typically by about 1% (for a total sensitivity of -6%).

When necessary, the polarization response can be accounted for with either laboratory characterization or in-field polarimetric calibration. The first option is usually sufficient, since the instrument polarization response does not change significantly with time or deployment conditions (as long as the optical system is unchanged). Polarimetric calibrations in the field would in many ways be the best solution but may be impractical. For example, although the emission port window is easily replaced with a wire-grid polarizer, the increased reflection of instrument emission back toward the detector degrades the instrument sensitivity (and cooling the polarizer and instrument is usually unreasonable). Polarimetric measurements with imaging or wide-field-of-view radiometers are especially troublesome (Shaw and Descour 1995), although such difficulties can be reduced by designing the optical system specifically for polarimetric measurements (Iannarilli et al. 2000).

5. Conclusions

The combination of emitted and reflected radiance components produces a partially polarized input signal for radiometers that view the sea surface. This polarization results in radiometric errors when the radiometer is sensitive to polarization. FTIR spectroradiometers tend to have such polarization sensitivity; the instrument considered here has a response that favors vertical polarization by about 5% (with an added approximately 1% when a beam-steering mirror is used). Thus, it is clear that the growing popularity of FTIR spectroradiometers creates an especially strong motivation for in-

cluding polarization in radiometric error budgets. Situations in which the instrument views the water at large incidence angles under a clear sky can require compensation of the instrument polarization response; situations with lower degrees of polarization in the scene should not require any treatment other than a calculation of the effect for inclusion in the error budget.

Acknowledgments. I appreciate useful comments and suggestions from Yong Han (University of Colorado, CIRES/NOAA), Edward Walsh (NASA guest worker at NOAA/ETL), and two anonymous reviewers.

REFERENCES

- Anderson, G. P., S. A. Clough, F. X. Kneizys, J. H. Chetwynd, and E. P. Shettle, 1986: AFGL atmospheric constituent profiles (0–120 km). Air Force Geophysics Laboratory Tech. Rep. AFGL-TR-86-0110. [NTIS AD A175173.]
- Cooper, A. W., W. J. Lentz, and P. L. Walker, 1996: Infrared polarization ship images and contrast in the MAPTIP experiment. *Proc. SPIE*, **2828**, 85–96.
- Donlon, C. J., and Coauthors, 1998: Solid-state radiometer measurements of sea surface skin temperature. *J. Atmos. Oceanic Technol.*, **15**, 775–787.
- Egan, W., 2000: Optical enhancement of aircraft detection using polarization. *Proc. SPIE*, **4133**, 172–178.
- Fetrow, M. P., S. H. Sposato, K. P. Bishop, and T. R. Caudill, 2000: Spectral polarization signatures of materials in the LWIR. *Proc. SPIE*, **4133**, 249–260.
- Gigioli, G. W., and T. S. Pagano, 1999: AIRS instrument response: Measurement methodology. *Proc. SPIE*, **3759**, 279–291.
- Howe, J. D., M. A. Miller, R. V. Blumer, T. E. Petty, M. A. Stevens, D. M. Teale, and M. H. Smith, 2000: Polarization sensing for target acquisition and mine detection. *Proc. SPIE*, **4133**, 202–213.
- Iannarilli, F. J., J. A. Shaw, S. H. Jones, and H. E. Scott, 2000: A snapshot LWIR hyperspectral polarimetric imager for ocean surface sensing. *Proc. SPIE*, **4133**, 270–283.
- Knight, E. J., C. Merrow, and C. Salo, 1999: Interaction between polarization and response vs. scan angle in the calibration of imaging radiometers. *Proc. SPIE*, **3754**, 308–319.
- Millikan, R. A., 1895: A study of the polarization of the light emitted by incandescent solid and liquid surfaces. *Phys. Rev.*, **3**, 81–99 and 177–192.
- Minnett, P. J., R. O. Knuteson, F. A. Best, B. J. Osborne, J. A. Hanafin, and O. B. Brown, 2001: The marine-atmospheric emitted radiance interferometer: A high-accuracy, seagoing infrared spectroradiometer. *J. Atmos. Oceanic Technol.*, **18**, 994–1013.
- Pagano, T. S., H. H. Aumann, K. Overoye, and G. Gigioli, 2000: Scan-angle radiometric modulation due to polarization for the Atmospheric InfraRed Sounder (AIRS). *Proc. SPIE*, **4135**, 108–116.
- Revercomb, H. E., H. Buijs, H. B. Howell, D. D. LaPorte, W. L. Smith, and L. A. Sromovsky, 1988: Radiometric calibration of IR Fourier transform spectrometers: Solution to a problem with the High-Resolution Interferometer Sounder. *Appl. Opt.*, **27**, 3210–3218.
- Sandus, O., 1965: A review of emission polarization. *Appl. Opt.*, **4**, 1634–1642.
- Schluessel, P., W. J. Emery, H. Grassl, and T. Mammen, 1990: On the bulk skin temperature difference and its impact on satellite remote sensing of sea surface temperature. *J. Geophys. Res.*, **95**, 13 341–13 356.
- Shaw, J. A., 1999: Degree of linear polarization in spectral radiances from water-viewing infrared radiometers. *Appl. Opt.*, **38**, 3157–3165.
- , 2001: Polarimetric measurements of long-wave infrared spectral radiance from water. *Appl. Opt.*, in press.
- , and M. R. Descour, 1995: Instrument effects in polarized infrared images. *Opt. Eng.*, **34**, 1396–1399.
- , H. M. Zorn, J. J. Bates, and J. H. Churnside, 1999: Observations of downwelling infrared spectral radiance at Mauna Loa, Hawaii, during the 1997–1998 ENSO event. *Geophys. Res. Lett.*, **26**, 1727–1730.
- Smith, W. L., and Coauthors, 1996: Observations of the infrared radiative properties of the ocean—Implications for the measurement of sea surface temperature via satellite remote sensing. *Bull. Amer. Meteor. Soc.*, **77**, 41–51.
- Suarez, M. J., W. J. Emery, and G. A. Wick, 1997: The multichannel infrared sea truth radiometric calibrator (MISTRIC). *J. Atmos. Oceanic Technol.*, **14**, 243–253.
- Wu, X., and W. L. Smith, 1997: Emissivity of rough sea surface for 8–13 μm : Modeling and verification. *Appl. Opt.*, **36**, 2609–2619.
- Zeisse, C. R., C. P. McGrath, and K. M. Littfin, 1999: Infrared radiance of the wind-ruffled sea. *J. Opt. Soc. Amer.*, **A16**, 1439–1452.